Hindawi
Advances in Civil Engineering
Volume 2022, Article ID 5985165, 13 pages
https://doi.org/10.1155/2022/5985165

Research Article

Numerical Simulation of Large Compression Deformation Disaster and Supporting Behavior of Deep Buried Soft Rock Tunnel with High In Situ Stress Based on CDEM

Hao Tang,[1,2,3] **Xiang Ji**,[1,2] **Hongyi Zhang**,[4] **and Tianbin Li**[1,2]

[1]*College of Environment and Civil Engineering, Chengdu University of Technology, Chengdu, Sichuan 610059, China*
[2]*State Key Laboratory of Geohazard Prevention and Geoenvironment Protection, Chengdu University of Technology, Chengdu, Sichuan 610059, China*
[3]*Sichuan Expressway Construction and Development Group Co. Ltd, Chengdu, Sichuan 610041, China*
[4]*Sichuan Mianjiu Expressway Co. Ltd, Chengdu, Sichuan, China*

Correspondence should be addressed to Tianbin Li; ltb@cdut.edu.cn

Received 18 October 2021; Revised 9 January 2022; Accepted 11 January 2022; Published 3 March 2022

Academic Editor: Qian Chen

Large compressive deformation of tunnels is a phenomenon involving plastic deformation and failure of surrounding rocks and often refers to the weak surrounding rock self-bearing capacity loss or partial loss. This research discusses the formation and evolution of large compressive deformation and effectiveness of the combined support of high in situ stress tunnel. From the new perspective of large deformation disaster caused by the structural failure of high in situ stress surrounding rock to clarify it, this paper illustrates the mechanism of progressive cracking and large deformation of high in situ stress soft rock tunnel from the aspects of the formation of self-bearing system, deformation evolution of the surrounding rock, mechanical properties of the surrounding rock, and failure characteristics. Accordingly, the continuous and discontinuous numerical simulation methods are used. The following conclusions are drawn by comparing the simulation results of surrounding rock under combined support with no support. (1) The supporting structure constitutes the self-supporting system with the surrounding rock and plays the roles of codeformation and load-bearing. (2) The support structure has evident reinforcing effect on the rock mass in the relaxation zone, thereby leading to the phenomenon of weakened rock mass failure. Moreover, the shear area develops to the compaction zone. (3) The supporting structure improves the bearing capacity of rock mass in the relaxation zone. It also increases the surrounding rock stress and reduces the range of the compaction zone. Simulation results verify that the combined support measures have a good suppression effect on the large compressive deformation, thereby providing a reference for similar projects and research on the large compressive deformation of soft rock.

1. Introduction

The continuous development of national highway construction and highway grade has resulted in the daily increase in the construction scale and number of highway tunnels. However, considering the constraints of geological conditions, planning requirements, and environmental protection, some tunnels have to be built in areas where the surrounding rock is weak and structurally developing. Thus, these tunnels' surrounding rock lacks sufficient strength and self-stabilizing capacity, and peripheral convergence and vault subsidence displacement are relatively large. Thereafter, selecting reserved deformation in accordance with specifications often leads to intrusion limits and replacement of arch frame. This outcome will cause secondary disturbance to the surrounding rock, thereby affecting the stability of the surrounding rock, and also delay the construction period, resulting in hidden safety hazards.

At present, there are no clear and unified criteria for the large deformation of surrounding rock. Some scholars have indicated that large deformation happens when the surrounding rock deformation exceeds the specified amount

[1, 2]. Others have defined large deformation by whether the deformation of the surrounding rock exceeds the reserved deformation [3]. Scholars' deepening research have indicated that large deformation could not be defined solely by the extent of deformation. Hence, large deformation is a type of plastic failure, and progressive and evident time effect was proposed [4–7]. Furthermore, a new definition of large deformation of surrounding rock was proposed according to the geological conditions and mechanical mechanism [8].

Research directions of large tunnel deformation mainly include tunnel surrounding rock convergent deformation mechanism [9–12], prediction of surrounding rock convergent deformation [13], and risk evaluation of large deformation [14]. In numerical simulation, the finite element method is used for the numerical simulation of large deformation supporting measures [15], research on response of tunnelling form to tunnel deformation [16], treatment of large deformation of soft broken surrounding rock [17], and research on the influence of large deformation on tunnel excavation [18]. Scholars have used the finite difference numerical simulation method as basis in conducting rock mass deformation analysis [19], studied the damage evolution of tunnels' secondary lining under the combined action of initial support corrosion and surrounding rock creep [20], and analysed the convergence deformation mechanism of tunnel excavation in composite stratum [21]. On the basis of combined finite-discrete element method (FDEM), which is a numerical simulation method, the failure and swelling deformation of soft surrounding rock was simulated [22]. Han et al. [23] studied the critical roles of the location and the dip angle of the fault in determining the rockburst development around the tunnel. Scholars have used the continuous discontinuous element method (CDEM), which is a simulation method, to conduct comparative studies on different support measures [24] and simulate the progressive failure process of tunnel lining under different water pressure conditions [25]. Yang et al. [26] simulated the evolution of stress and fracture in tunnel excavation. Feng et al. [27, 28] discussed the macroscopic mechanical properties of brittle soil-rock mixture materials and realized the accurate calculation of rock mass explosive force and description of rock mass damage and fracture process through CDEM. Meanwhile, CDEM has been used in seismic stability analysis of bedding slope, damage and fracture process of rocks under explosion load, and progressive failure process of rock and soil medium under impact load [29, 30]. However, CDEM has been rarely used in large deformation of tunnel surrounding rock. Previous studies on large deformation have been conducted mostly from the continuous perspective, such as deformation amount and stress field characteristics, without considering the influence of structural failure on large deformation and the interpretation of discontinuous process. Therefore, CDEM should be introduced to substantially simulate the progressive failure process of large deformation disasters.

In terms of supporting measures, conventional measures for surrounding rock with a certain load-bearing capacity include shotcrete support, bolt support, steel arch support, and advanced small pipe support. However, joint support measures have been commonly used in projects. For considerably developed rock masses, such as extreme fracture, fault fracture and squeezed rock zones, and extremely weak layer, conventional support measures occasionally fail. Thus, a special support measure must be adopted. For example, constant resistance large deformation bolt [31] absorbs the deformation energy of rock mass through the three stages of elastic deformation, structural deformation, and ultimate deformation. Hence, energy in the surrounding rock is completely released to a stable state. Small-diameter anchor cable [32] restricts large deformation through friction between the grouting body in the external anchorage section and bore wall and the suspension anchoring effect of the point anchor. Steel fiber shotcrete [33] is made of ordinary concrete mixed with steel fiber to achieve the functions of crack resistance, reinforcement, and toughness. Wu et al. [34] proposed a new reinforcement support system that combines filler wall, shotcrete, grouting cable, prestressed anchorage, and U-shaped steel support. However, only a few studies on the effectiveness of various supporting measures have explained the effectiveness of supporting measures from the perspective of the impact of structural damage of surrounding rocks on large deformation disasters and supporting structures.

Therefore, this study uses the preceding problems as bases in taking the construction of the Jiumian High-speed Baima Tunnel as research background and utilizes CDEM to simulate the large deformation disaster of high in situ tunnel and combined support measures. The forming and evolution mechanism of large deformation of high-stress tunnel and the effectiveness of combined support are discussed from the new perspective of large deformation disaster caused by the structural failure of high-stress surrounding rock.

2. Overview of Surrounding Rock Self-Supporting System and Large Squeezing Deformation

The occurrence of squeezing large deformation disaster is characterized by the significant deformation and failure of surrounding rocks. Figure 1 shows such examples as deformation and distortion of steel arch, cracking of shotcrete, spalling, initial support invasion limit, vault settlement, side wall extrusion, and floor heave. To explore the internal mechanism based on these typical large-deformation external failure phenomena, actual engineering should be used as a background, combined with numerical simulation, and the formation and evolution mechanism of large-deformation based on the theoretical results obtained from previous studies must be analysed and clarified.

Therefore, the current study uses Baima Tunnel as engineering background to study the formation, development, and failure process of large squeezing deformation and the state of the surrounding rock self-supporting system when the large squeezing deformation of soft rock occurs. On the basis of self-supporting system of surrounding rock, combined with the results of numerical simulation, the mechanism of large squeezing deformation is clarified from the

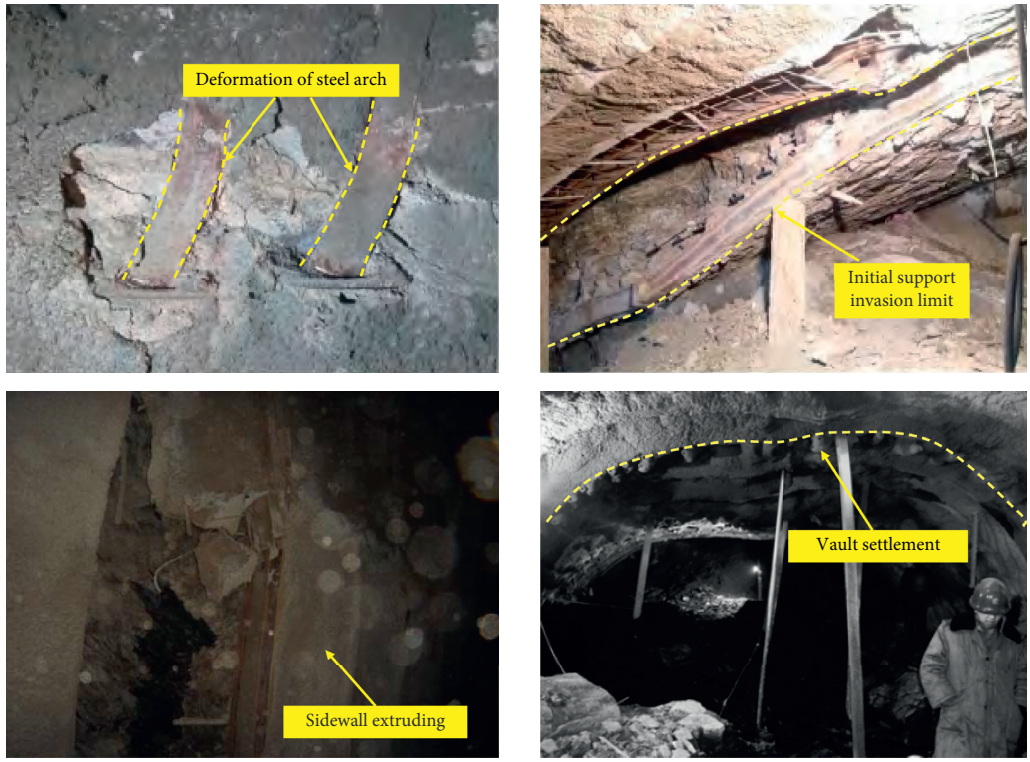

Figure 1: Typical failure characteristics of large deformation.

formation of surrounding rock self-supporting system, evolution of surrounding rock deformation, evolution of the mechanical behavior of rock mass, and failure characteristics.

The self-supporting system of surrounding rock [35] refers to the deformation of surrounding rock owing to stress adjustment during tunnel excavation. When the deformation of the surrounding rock converges and reaches a stable state, a self-supporting system structure is formed inside the surrounding rock to bear the pressure of the surrounding rock. The surrounding rock deformation of a tunnel is divided into the relaxation, compaction, and original stress zones from the inside to the outside of the tunnel wall (see Figure 2(a)). Relaxation zone refers to the tensile deformation of a certain range of rock mass around the cavern. Compaction zone refers to the area where the rock mass is in a state of compressive deformation in a certain deep part around the tunnel. The original rock stress zone is the area where the rock mass is in the original rock stress state. When the internal stress of the rock mass is dominated by horizontal tectonic stress, the original compaction zone will evolve into a stress-bearing arch at the top and bottom and a zone where stresses on the left and right sides expand and release to the deep from a horizontal perspective (see Figure 2(b)).

Therefore, the formation mechanism of the large deformation of the surrounding rock self-supporting system can be summarized as when the rock mass around the tunnel wall undergoes tensile deformation and fails to form a relaxation zone. During stress adjustment and redistribution, the rock mass at the deep part of the surrounding rock undergoes tangential compression to form compaction and original rock stress zone. However, under the influence of such factors as high tectonic stress, structural cracking, and strength characteristics of soft rock, the self-supporting capacity of the rock mass in the relaxation zone is lost, further development of deformation and failure cannot be converged, and the self-supporting system of the surrounding rock fails, thereby ultimately leading to large deformation disasters.

3. Numerical Simulation of Large Compression Deformation Mechanism of Soft Rock in Tunnel

CDEM is based on the Lagrange equation to realize the coupling of finite and discrete elements and simulate the internal and boundary fractures of the block to realize the progressive failure process of the material by block representing the continuous properties and interface representing the discontinuous properties (see Figure 3). The GDEM software used in this study is based on CDEM to simulate the entire dynamic process of block from continuous deformation to fracture movement. GDEM has certain advantages compared with the commonly used finite element and discrete element software. GDEM can describe the nonlinear mechanical behavior of rock mass deformation and failure under high in situ stress, solve nonlinear and dynamic unstable problems using explicit calculation method, and simulate large deformation failure process through the block boundary and internal fracture. GDEM is capable of GPU

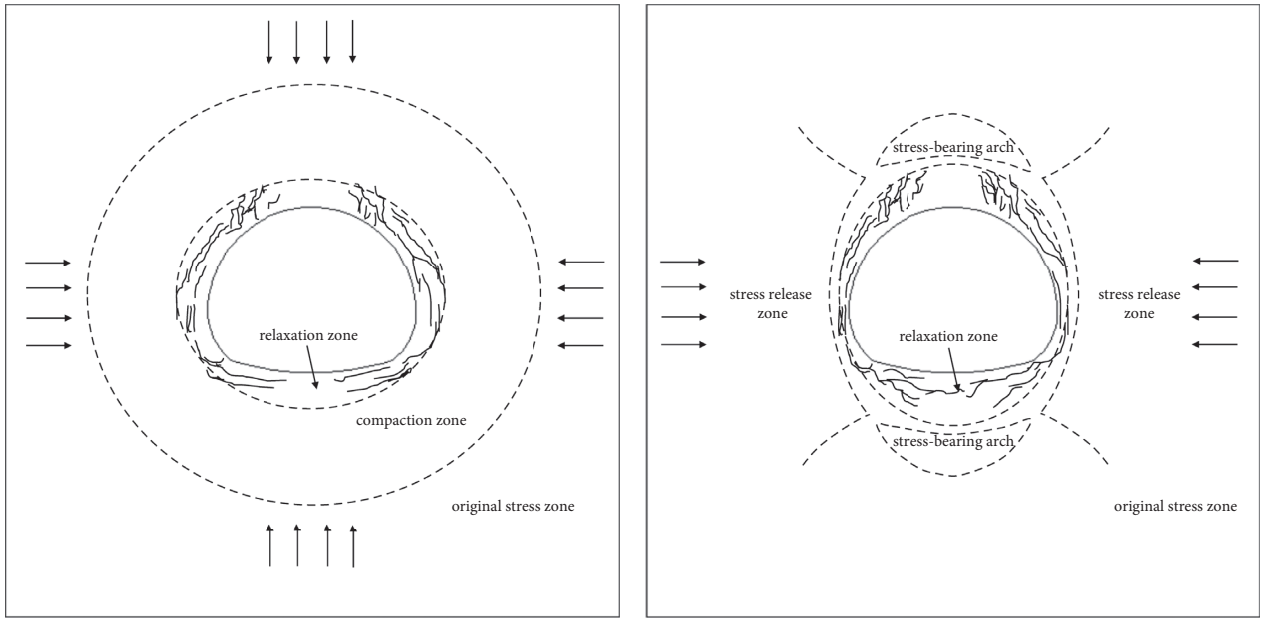

Figure 2: Schematic of the surrounding rock self-supporting system. (a) Horizontal and vertical tectonic stress. (b) Horizontal tectonic stress.

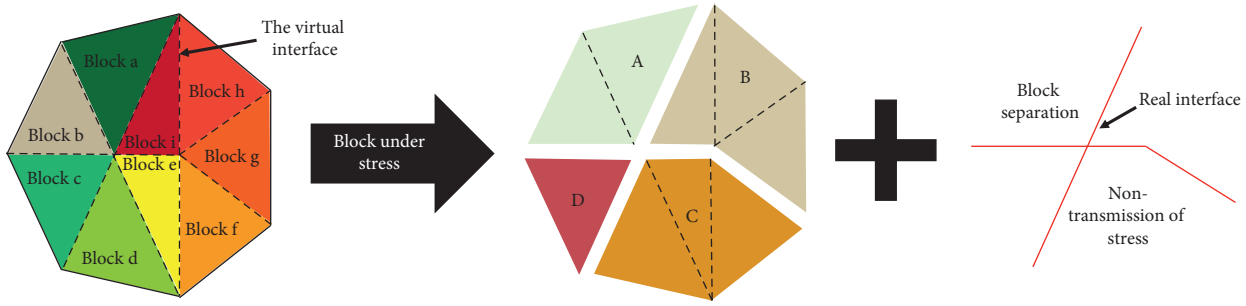

Figure 3: Block and interface diagram of CDEM [28].

and CPU parallel acceleration and can be equipped with various core modules of numerical computation, which can be integrated and managed.

3.1. Large Deformation Numerical Simulation Scheme Based on CDEM. This study designed two simulation schemes to significantly clarify the mechanism of large extrusion deformation and support effect: (1) large section excavation A without support measures and (2) large section excavation B with combined support measures. The significance of the two simulation schemes is to compare the formation process of the surrounding rock self-supporting system without support measures and the timely adoption of combined support measures. Scheme A aims to clarify the formation and evolution mechanism of large compression deformation. Scheme B is designed to compare support effect from the perspectives of deformation, rock mass mechanical behavior changing process, and failure characteristics. Deformation of rock mass was analysed from vault settlement, floor uplift, and surrounding convergent displacement, while the original contour line of the tunnel was used to clearly compare deformation changes. Therefore, displacement monitoring points of the tunnel contour line are arranged, as shown in Figure 4. The mechanical behavior of the surrounding rock is reflected in the stress cloud map, and the formation of the self-bearing system of surrounding rock is observed. Lastly, the failure properties and characteristics of the surrounding rock are analysed using the failure type diagram.

This study uses GDEM-BlockDyna in numerical simulation to simulate large compression deformation. The model is based on the K39 + 714–726 section of the left inclined shaft of Baima Tunnel, and the size of the calculation model is 50 m × 50 m. The specific model size and monitoring point layout are shown in Figure 4. The specific model size of plan B is shown in Figure 5. The linear elastic constitutive model is selected as the constitutive model of the solid unit, and the Mohr-Coulomb strain softening model is adopted for the contact surface. In the elastic-plastic

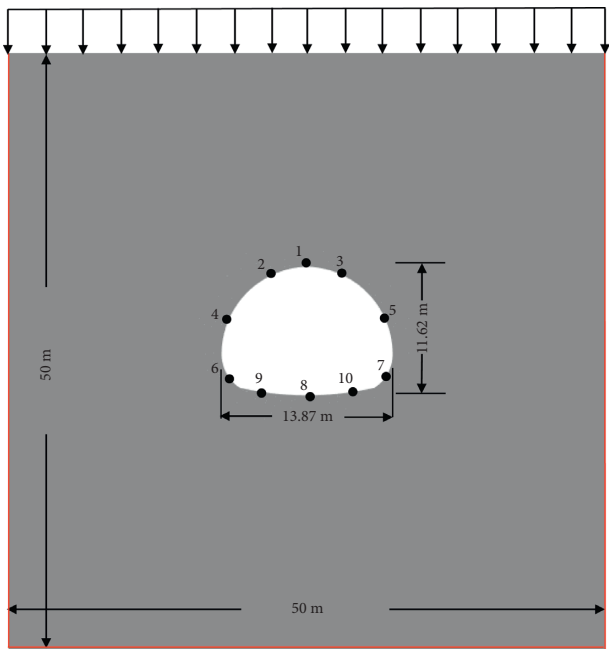

Figure 4: Model size diagram of the model without support.

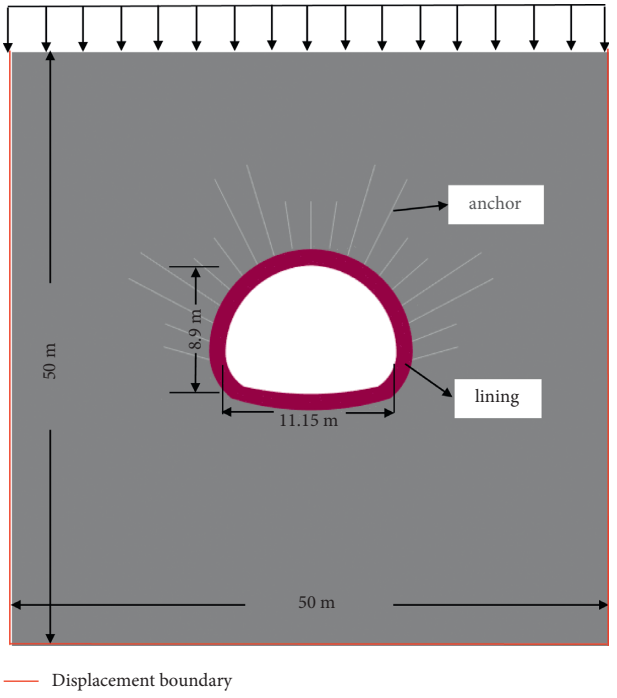

Figure 5: Model size diagram of the combined support measures.

calculation, displacement constraints are imposed on the left, right, and lower boundaries of the model, and the stress constraints are imposed on the upper part of the model. Vertical force of the overlying rock mass on the upper part of the model is applied in the form of uniformly distributed load. Thereafter, three-dimensional normal stress and shear stress are applied to each block to simulate structural stress. Displacement and velocity generated in the elastic-plastic calculation are cleared, and stress boundary conditions of the model are changed to viscous boundary conditions. The reason is that viscous boundary will absorb stress, thereby avoiding false reflection of the stress wave, and dynamic calculation is performed.

Baima Tunnel is located at the junction of Pingwu County and Jiuzhaigou County in Sichuan Province. This tunnel is a dominant engineering of the highway from Jiuzhaigou (Sichuan-Gansu boundary) to Mianyang. The geological structure of the tunnel is complex. That is, the lithology is mainly slate and phyllite, and the uniaxial saturated compressive strength of the rock is mostly below 30 MPa. Hence, Baima Tunnel is a typical soft rock tunnel. Faults in this area are relatively developed, with 6 faults intersecting the tunnel body, and the surrounding rocks of grades IV and V account for approximately 90% of the tunnel length. The tunnel is in a section dominated by slate, and the surrounding rock is dominated by grade V. Based on the actual surrounding rock exposure of the K39 + 714–726 section of the left line of the inclined shaft of the tunnel, rock mechanics, anchor, and lining parameters of large deformation simulation are shown in Table 1. Ground stress parameters are presented in Table 2.

3.2. Analysis of the Simulation Results of Large Compression Deformation without Support

3.2.1. Deformation Evolution of the Surrounding Rock. Figure 6 shows the displacement cloud map, in which the white-dotted line is the original contour line of the tunnel. By comparing the original contour line, the deformation of the surrounding rock is evidently reflected. This study analyses the deformation characteristics from vault settlement, floor uplift, and surrounding convergent displacement.

The maximum cumulative displacement data of monitoring points are shown in Figure 7. As soon as the excavation is completed, the surrounding rock immediately deforms because excavation leads to the redistribution of surrounding rock stress, and the strength of soft rock itself is weak. In the absence of support conditions, the rebound caused by stress release process and dilatation caused by stress adjustment open the originally closed structural plane of the rock mass. Therefore, from 0 to 30,000 steps, the maximum displacement of the vault settlement increases to 175 mm, surrounding convergent displacement increases to 222 mm, and floor uplift reaches 344 mm. From 40,000 to 310,000 steps, the overall displacement of the surrounding rock enters a stable stage, maximum settlement displacement of the vault is 189 mm, surrounding convergence displacement is 233 mm, and displacement of floor uplift is 357 mm. At this time, the surrounding rock is in a state of temporary stability, but further attrition crushing of surrounding rock further reduces the strength of the rock mass. Consequently, from 320,000 to 340,000 steps, the maximum cumulative settlement displacement of the vault increases by 17 mm, maximum surrounding convergent displacement increases by 25 mm, and maximum floor uplift displacement

Table 1: Parameters of large deformation simulation.

	Density of material (kg/m^3)	Modulus of elasticity (GPa)	Poisson's ratio	Cohesive forces (MPa)	Tensile strength (MPa)	Angle of internal friction (°)
Rock	2346	2.6	0.35	25	25	27
Lining	2300	3.0	0.3	27	27	30
Anchor	7800	10	0.25	500	500	75

Table 2: In situ stress parameters for large deformation simulation.

Stress component (MPa)					
δ_x	δ_y	δ_z	τ_{xy}	τ_{yz}	τ_{xz}
40.94	25.15	41.08	3.38	3.5	1.7

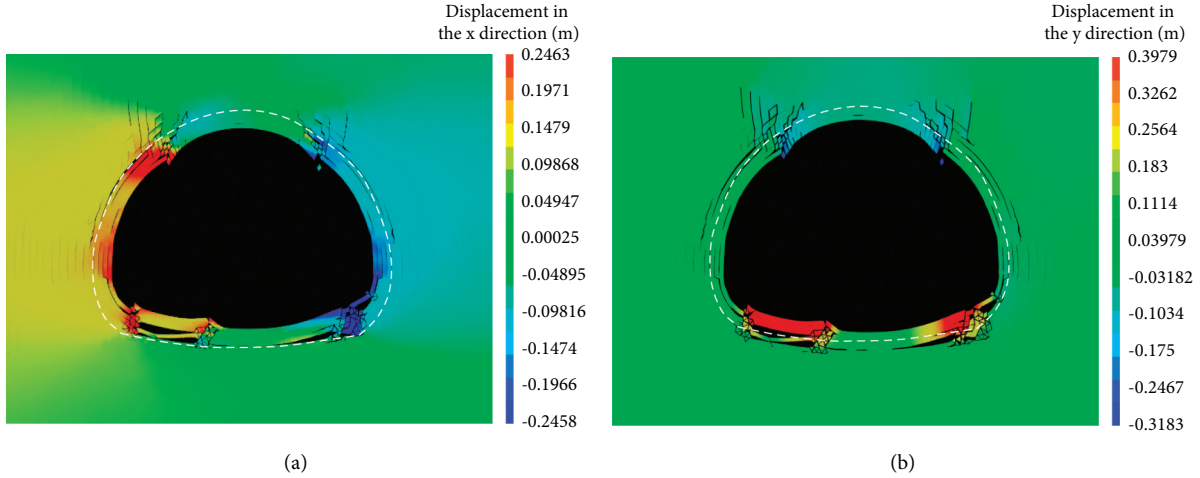

Figure 6: Displacement cloud maps. (a) X-direction displacement. (b) Y-direction displacement.

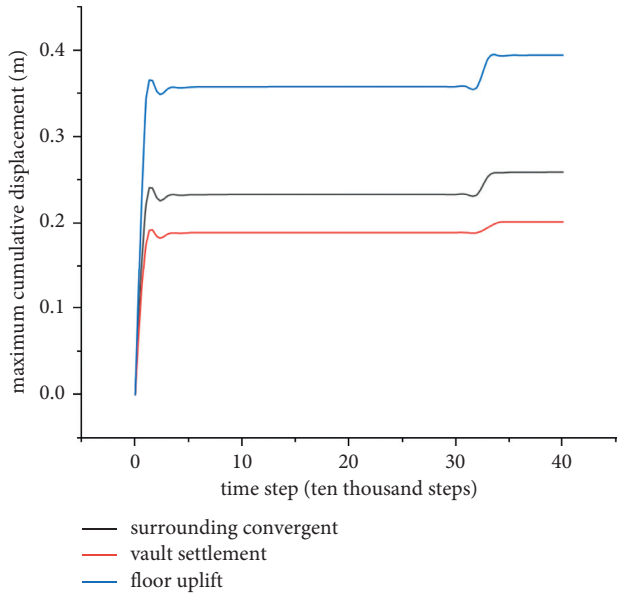

Figure 7: Maximum cumulative displacement of the tunnel contour.

increases by 37 mm. Lastly, large compression deformation occurs.

The deformation characteristics of soft rock with high stress are summarized as follows: (1) The occurrence of large compression deformation with soft rock is instantaneous. (2) Crushing of soft rock will change the stable stress state of rock mass and reduce the strength of rock mass, leading to the occurrence of large deformation disaster when deformation is temporarily stabilized.

3.2.2. Mechanical Behavior Evolution Surrounding Rock. Given that the simulated objects are mainly subjected to horizontal tectonic stress, the horizontal stress cloud maps of 20,000 and 420,000 steps and large principal stress cloud maps are selected. In the stress cloud diagram, tension is positive and pressure is negative. The entire surrounding rock is under pressure. According to the self-bearing system of the surrounding rock, the formation of compaction zone is the result of the change of large principal stress to tangential direction along the tunnel and numerical increase. In Figure 8, the surrounding rock mass in a certain range is

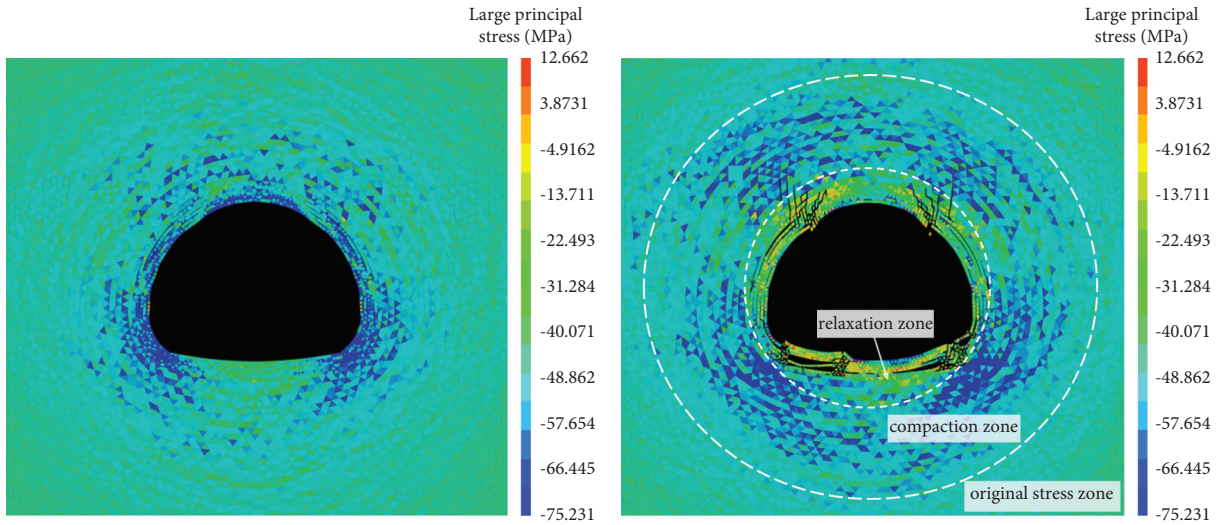

Figure 8: Cloud diagram of the large principal stress. (a) 20,000 steps. (b) 420,000 steps.

subjected to tangential compression, and the large principal stress forms a region distributed along the tangential direction of the tunnel. Meanwhile, the stress and range of this area gradually increase to form a compaction zone. The surrounding rock breaks owing to extrusion, cracks expand, and relaxation zones are formed. Stress of the compaction zone is larger than the original rock stress, and the original rock stress is greater than the relaxation zone. The reason is that the rock mass of the compaction zone is under confining pressure and its ultimate strength increases with an increase in confining pressure. Owing to the excavation, the rock mass in the relaxation zone changes from a three-way stress state to a two-way stress state, resulting in tensile failure. However, owing to friction, viscosity, and mutual mosaic among rocks, the rock mass in the relaxation zone continues to have integrity, which can provide resistance constraints to the rock mass in the compaction zone.

Relaxation, compaction, and original rock stress zones are formed in the horizontal stress cloud map (Figure 9), and the compaction zone is transformed into stress bearing arch and stress release zone in the horizontal stress cloud map. When the surrounding rock is mainly subjected to horizontal tectonic stress, rock mass in the compaction zone of the vault and arch bottom will have substantially high bearing capacity because of tangential compression and confining pressure. Thus, stress distribution similar to the arch, called stress-bearing arch, is formed. With the gradual formation of relaxation zone on the left and right sides of the tunnel, stress is constantly adjusted and gradually expanded and released to the deep rock mass, forming the stress release zone.

The mechanical behavior of large compression deformation of soft rock with high stress can be summarized as follows: (1) Stress of compaction zone is larger than the original rock stress, and the original rock stress is greater than the relaxation zone. (2) Rock mass in the relaxation zone has integrity and can provide certain resistance constraints to the rock mass in the compaction zone. (3) When the surrounding rock is mainly subjected to horizontal tectonic stress, the compaction zone will form stress-bearing arch and stress release zone.

3.2.3. Failure Characteristics. Figure 10 shows the failure types of large compression deformation (0, undamaged; 1, current tensile failure; 2, current shear failure; 4, past tensile failure; and 8, past shear failure). After excavation, the shallow surface of the surrounding rock is gradually cracked, such as a few cracks along the contour line of the tunnel appearing at the left and right arch shoulders (Figure 10(a)). Then, shear failure blocks are mainly concentrated in the shallow surface of surrounding rock (Figures 10(b) and 10(c)). Furthermore, cracks extended towards the vault to form vertical cracks, and cracks in the bottom floor developed through, leading to the formation of the relaxation zone (Figure 10(d)). As the surrounding rock is strongly crushed by structural compression, the spalling and block dropping phenomenon occurs in the arch shoulder, and the floor is uplifted owing to the connection of cracks in the arch bottom, and self-bearing capacity of the relaxation zone is gradually lost and large deformation occurs. The relaxation zone is mainly tensile failure, while the compression zone is shear failure. By comparing Figures 10(c) and 10(d), the shear failure zone of the surrounding rock clearly extends from the relaxation zone to the deep part of the compaction zone. Moreover, shear failure gradually occurs in the compaction zone in the gradual formation of the relaxation zone, as well as gradual loss of the self-bearing capacity of the relaxation zone and gradual formation of the shear failure of the rock mass in the compaction zone. The reason is that, after excavation, the rock mass around the tunnel moves towards the tunnel clearance surface, resulting in tensile deformation and tensile failure. The self-bearing capacity of the rock mass in the relaxation zone gradually is lost, and

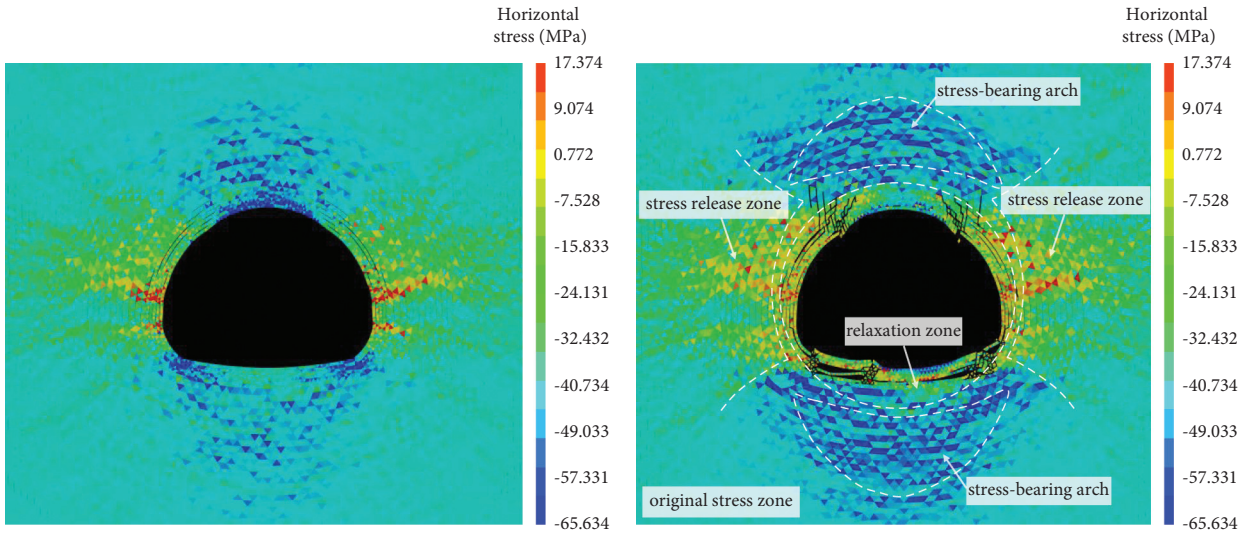

Figure 9: Horizontal stress cloud diagram. (a) 20,000 steps. (b) 420,000 steps.

stress is redistributed. Consequently, the rock mass in the compaction zone is further subjected to tangential compression and shear failure occurs.

3.3. Study on the Effectiveness of the Simulation of Combined Support Based on CDEM

3.3.1. Deformation Evolution of the Surrounding Rock. The maximum cumulative displacement data of the monitoring point are shown in Figure 11. Compared with the no support condition, the maximum cumulative displacement of vault settlement is reduced by 22.3%, maximum convergence displacement is reduced by 18.5%, and maximum displacement of floor uplift is reduced by 47.7%. These results indicate that support structure strengthens the rock mass in the relaxation zone, and the self-supporting system formed by the support structure and surrounding rock relatively inhibits the surrounding rock deformation. Compared with the condition without support, the stable period increases because the existence of support structure delays the occurrence of large deformation. At 390,000–400,000 steps, the maximum cumulative settlement displacement of vault, periphery convergence, and floor uplift increase suddenly. Compared with the sudden increase in surrounding rock deformation under the no support condition, the presence of support structure significantly reduces the strength reduction of soft rock caused by extrusion and crushing and makes the final convergence of deformation.

The simulation results indicate that the combined support structure has evident restraining effect on the surrounding rock deformation. The supporting structure and surrounding rock constituting the self-supporting system of surrounding rock play a role in strengthening rock mass in the relaxation zone and collaborative deformation. It not only prolongs the development period of large deformation, but also alleviates the crushing degree of surrounding rock due to extrusion, thus leading to the inhibitory effect on large deformation.

3.3.2. Mechanical Behavior Evolution Surrounding Rock. In the final horizontal stress cloud map that compares the no support (Figure 12(a)) with combined support (Figure 12(b)), the surrounding rock and supporting measures are generally compressed, and the supporting measures have an evident reinforcing effect on rock mass around the tunnel. The failure phenomenon of rock mass in the relaxation zone is alleviated and bearing capacity is improved, leading to the narrowing of the stress-bearing arch and stress release zone. At this time, the supporting structure and surrounding rock form a self-bearing system together and collaborate deformation. From the crack development state, under the condition of combined support, the crack only develops along the tunnel contour at the left and right shoulder but does not extend further to the arch bottom and waist, and the crack penetration at the arch bottom is effectively suppressed. The large principal stress cloud map indicates that, compared with the no support condition (Figure 13(a)), the increase in stress in the compacting zone and the relaxation zone and the trend of the compaction zone extending to the deep surrounding rock are obviously inhibited, which is in contrast to the expansion of the compaction zone to the depth of surrounding rock without support condition, indicating that the supporting structure participates in the load bearing of surrounding rock and shares part of the stress in the compacted zone.

In summary, the reinforcement effect of support structure on rock mass in the relaxation zone increases the bearing capacity and the stress of rock mass in the relaxation zone and decreases range in the compaction zone. The trend of the compaction zone extending to the deep surrounding rock is obviously inhibited. Moreover, the supporting

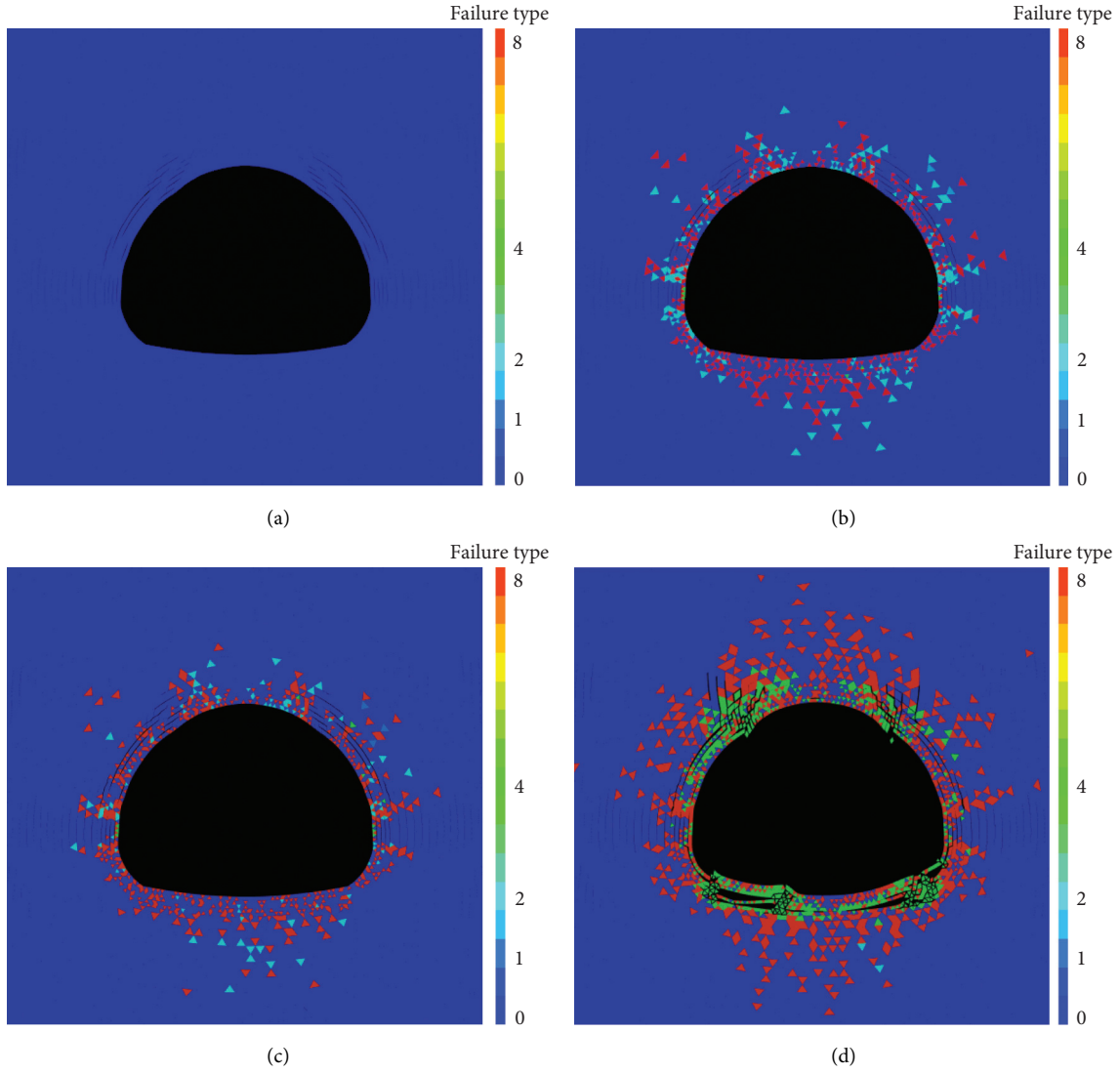

Figure 10: Diagram of the failure types. (a) 200,000 steps. (b) 300,000 steps. (c) 350,000 steps. (d) 420,000 steps.

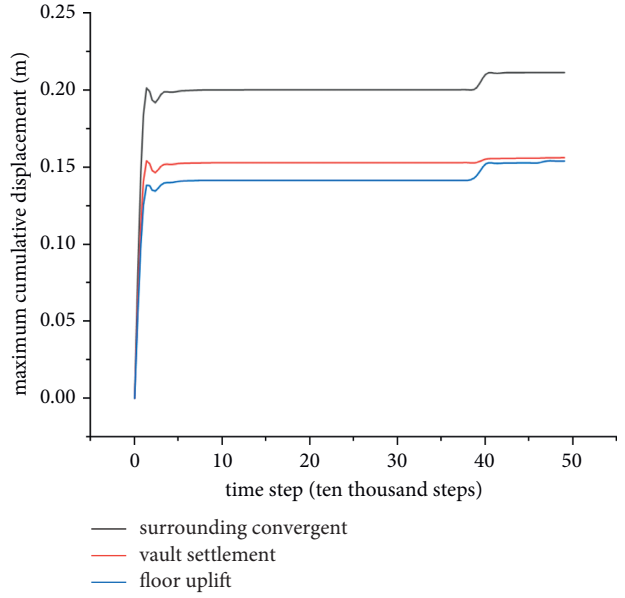

Figure 11: Maximum cumulative displacement of the tunnel contour.

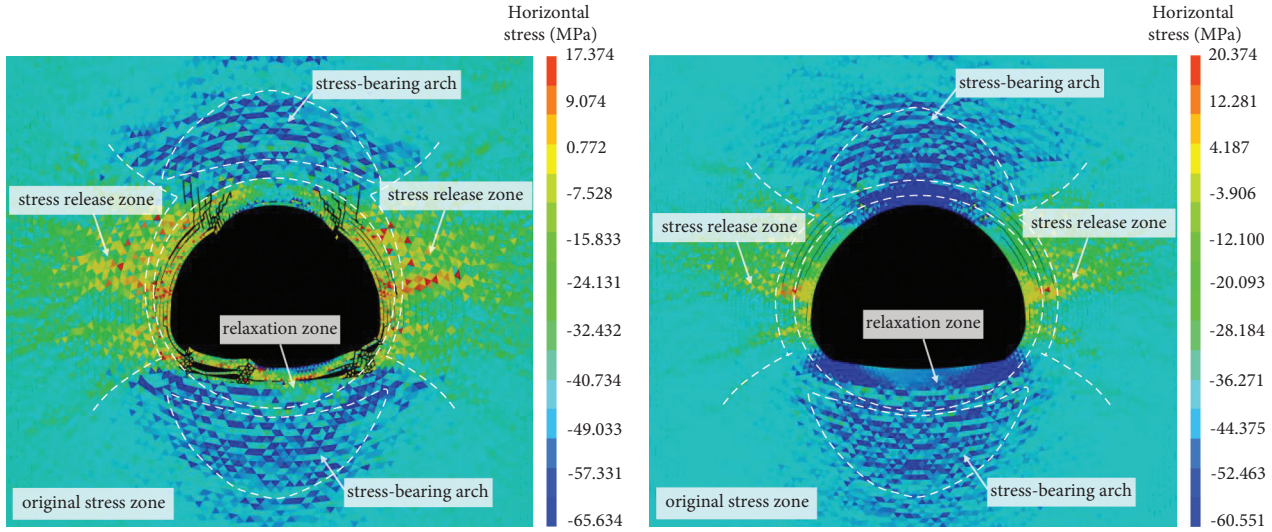

(a) (b)

Figure 12: Comparison of horizontal stress cloud images. (a) No support. (b) Combined support.

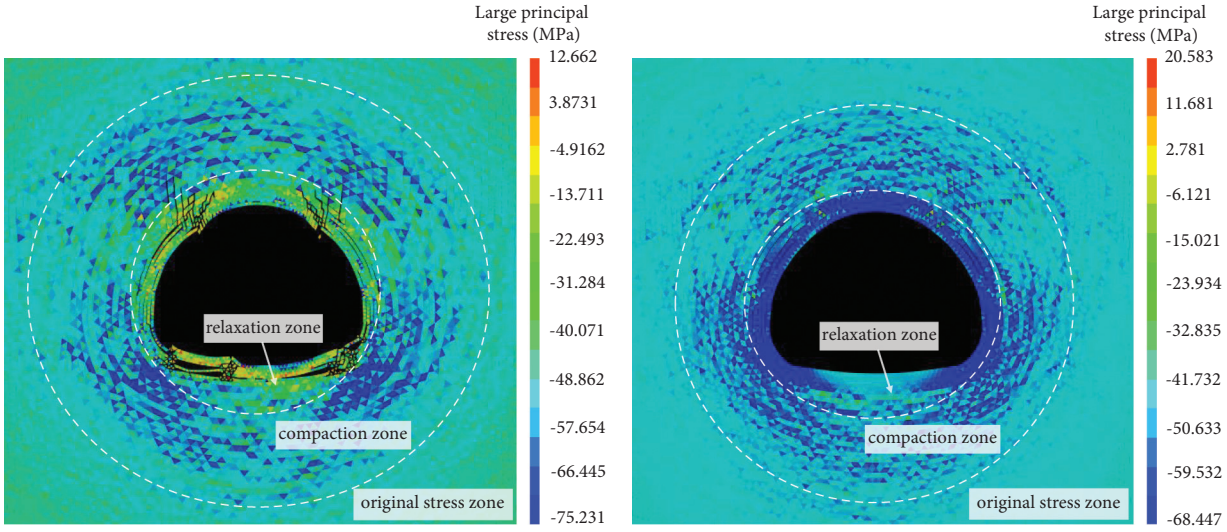

(a) (b)

Figure 13: Comparison of large principal stress cloud images. (a) No support. (b) Combined support.

structure and surrounding rock form a self-bearing system to bear the load.

3.3.3. Failure Characteristics. Figure 14 shows the comparison of the final failure types of no support and combined support measures (0, undamaged; 1, current tensile failure; 2, current shear failure; 4, past tensile failure; and 8, past shear failure). Some cracks along the tangential direction of the tunnel appear in the support structure and shallow surrounding rock. Some cracks along the tangential direction of the tunnel appear in the support structure and shallow surrounding rock. Furthermore, the main failure characteristics are shear failure and the phenomenon of tension failure in the relaxation zone has disappeared. Compared with the condition without support, the failure area of rock mass in the relaxation zone under the combined support measures is significantly reduced, and the number of cracks is also significantly suppressed, especially the failure phenomenon of the bottom of arch and the vault. The degree of rock mass fracture due to tectonic stress is obviously suppressed and the integrity of surrounding rock is effectively improved. Meanwhile, the shear failure area also expands deep in surrounding rock because the support structure strengthens the rock mass in the relaxation zone, resulting in the failure phenomenon developing to the compaction zone and deep surrounding rock. This result proves that the support structure and surrounding rock jointly form a self-supporting system to suppress the failure phenomenon.

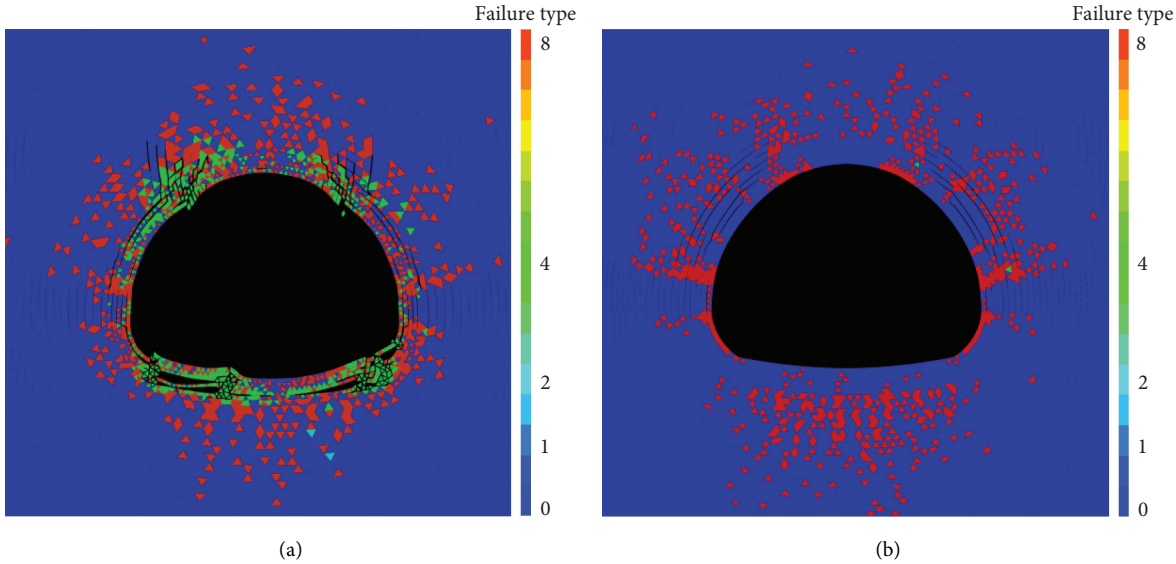

Figure 14: Diagram of failure types. (a) No support. (b) Combined support.

4. Conclusions

This study takes Baima Tunnel as background and compares the numerical simulation results of the two cases of unsupported and combined support measures. The following conclusions are drawn:

(1) The occurrence of large compressive deformation of soft rock with high in situ stress is instantaneous, and the further crushing of soft rock will change the stress stability state and reduce the strength of rock mass, leading to the occurrence of large deformation disasters.

(2) The stress of compaction zone is larger than the original rock stress, and the original rock stress is greater than the relaxation zone. Rock mass in the relaxation zone has integrity and can provide certain resistance constraints to the rock mass in the compaction zone. When the surrounding rock is mainly subjected to horizontal tectonic stress, the compaction zone will form stress-bearing arch and stress release zone.

(3) Tension and shear failures mainly occur in the relaxation and compaction zones, respectively. In the process of gradually losing the self-bearing capacity of the relaxation zone, the shear failure area of surrounding rock evidently extends from the relaxation zone to the deep compaction zone.

(4) The supporting structure and surrounding rock constitute the surrounding rock self-bearing system, which prolongs the development period of large deformation and alleviates the crushing degree of surrounding rock due to extrusion, thus leading to the inhibitory effect on large deformation.

(5) The supporting structure and surrounding rock constitute the surrounding rock self-bearing system, which strengthens the rock mass in the relaxation zone. Thus, the failure phenomenon of the rock mass in the relaxation zone is suppressed, bearing capacity is improved, stress in the compaction zone increases, and range of the compaction zone is reduced. The supporting structure plays a role in collaborative deformation and sharing the load together.

(6) With the support structure, the rock mass in the relaxation zone and the compaction zone is mainly shear failure. The degree of rock mass fracture due to tectonic stress is obviously suppressed and the integrity of surrounding rock is effectively improved. The shear failure area extends from relaxation zone to compaction zone and deep surrounding rock.

There are still some problems to be further discussed in this paper:

(1) In this paper, the quasi-static process of sudden unloading is adopted in the simulated excavation. However, in the actual excavation process of tunnel chamber, the mechanism of large compression deformation is under dynamic disturbance. Therefore, the mechanism of large compression deformation can be further studied from the perspective of static and dynamic load combined action.

(2) The simulation effect of large compression deformation depends on mesh division, which is untrue to some extent. So, a more appropriate numerical calculation model needs to be established from the optimization of model modelling and reduce reliance on mesh.

(3) The simulation process in this paper does not consider geological structure and other complex conditions, which requires further study.

Data Availability

The data used to support the findings of this study are available from the corresponding author upon request.

Conflicts of Interest

The authors declare that they have no conflicts of interest.

Acknowledgments

This paper was supported by the National Natural Science Foundation of China (nos. 41807255, 41772329, and U19A20111), the State Key Laboratory of Geohazard Prevention and Geoenvironment Protection Independent Research Project (SKLGP2020Z010), Sichuan Science and Technology Project (no. 2021YJ0041), and Transportation Science and Technology Project (2020-MS5-146).

References

[1] Z. M. Xu and R. Q. Huang, *Deep Buried Extra-long Tunnel and its Construction Geological Hazards*, p. 220, Southwest Jiaotong University Press, Shanghai, China, 2000.

[2] G. Z. Bian, "The criterion and treatment measures of large deformation of tunnel surrounding rock are discussed," *Science and Technology Bulletin*, no. 2, pp. 15–17, 1998.

[3] Y. Yu, "Serious deformation of surrounding rock in squeezing ground," *Modern tunnelling technology*, no. 1, pp. 46–51, 1998.

[4] Y. Jiang, Y. L. Li, and T. B. Li, "Study of the classified system of types and mechanism of great distortion in tunnel and underground engineering," *Geological hazards and environmental protection*, vol. 15, no. 4, pp. 46–51, 2004.

[5] C. H. Wang, P. Sha, and Y. F. Hu, "Study of Squeezing Deformation Problems during Tunneling," *Rock and Soil Mechanics*, vol. 32, no. A2, pp. 143–147, 2011.

[6] C. D. Martin, P. K. Kaiser, and D. R. Mccreath, "Hoek-Brown parameters for predicting the depth of brittle failure around tunnels," *Canadian Geotechnical Journal*, vol. 36, no. 1, pp. 136–151, 1999.

[7] B. Singh and R. K. Geol, *Rock Mass Classification: A Practical Approach in Civil Engineering*, Elsevier Science, Amsterdam, Netherlands, 1999.

[8] T. B. Li, Y. L. Li, and L. S. Wang, *Study on Mechanism, Prediction and Prevention of Large Deformation of Tunnel under High In-Situ Stress*, Chengdu University of Technology, vol. 22, no. A1, pp. 2405–2408, Chengdu, China, 2008.

[9] K. Wang, S. Xu, Y. Zhong, Z. Han, and E. Ma, "Deformation failure characteristics of weathered sandstone strata tunnel: a case study," *Engineering Failure Analysis*, vol. 127, Article ID 105565, 2021.

[10] C. Xu and C. Xia, "A new large strain approach for predicting tunnel deformation in strain-softening rock mass based on the generalized Zhang-Zhu strength criterion," *International Journal of Rock Mechanics and Mining Sciences*, vol. 143, Article ID 104786, 2021.

[11] A. Vrakas and G. Anagnostou, "A finite strain solution for the elastoplastic ground response curve in tunnelling: rocks with non-linear failure envelopes," *International Journal for Numerical and Analytical Methods in Geomechanics*, vol. 41, no. 7, pp. 1077–1090, 2017.

[12] K. H. Park, "Large strain similarity solution for a spherical or circular opening excavated in elastic-perfectly plastic media," *International Journal for Numerical and Analytical Methods in Geomechanics*, vol. 39, no. 7, pp. 724–737, 2015.

[13] C. Li, S. Hou, Y. Liu, P. Qin, F. Jin, and Q. Yang, "Analysis on the crown convergence deformation of surrounding rock for double-shield TBM tunnel based on advance borehole monitoring and inversion analysis," *Tunnelling and Underground Space Technology*, vol. 103, Article ID 103513, 2020.

[14] C. H. Bai, Y. G. Xue, D. H. Qiu, M. X. Su, X. M. Ma, and H. T. Liu, "Analysis of factors affecting the deformation of soft rock tunnels by data envelopment analysis and a risk assessment models," vol. 116, Article ID 10411, 2021.

[15] X F, *Numerical Simulation of Asymmetric Large-Deformation Energy-Releasing Bolt Support for Layered Soft Rock Tunnel*, Chengdu University of Technology, vol. 4, no. 2, pp. 1–125, Chengdu, China, 2020.

[16] Y. Hu, H. Y. Lei, G. Zheng et al., "Assessing the deformation response of double-track overlapped tunnels using numerical simulation and field monitoring," *Journal of Rock Mechanics and Geotechnical Engineering*, 2021, vol. 21, In Press.

[17] C. Pan, Z. Q. Feng, T. Liu, and W. Li, "A numerical simulation of the treatment for weak and broken rock tunnel of large deformation," *Journal of Guangxi University*, vol. 37, no. 1, pp. 141–146, 2012.

[18] D. Kim, "Large deformation finite element analyses in TBM tunnel excavation: CEL and auto-remeshing approach," *Tunnelling and Underground Space Technology*, vol. 116, no. 1, Article ID 104081, 2012.

[19] J. Luo, D. Zhang, Q. Fang, D. Liu, and T. Xu, "Mechanical responses of surrounding rock mass and tunnel linings in large-span triple-arch tunnel," *Tunnelling and Underground Space Technology*, vol. 113, Article ID 103971, 2021.

[20] G. Xu and M. Gutierrez, "Study on the damage evolution in secondary tunnel lining under the combined actions of corrosion degradation of preliminary support and creep deformation of surrounding rock," *Transportation Geotechnics*, vol. 27, Article ID 100501, 2021.

[21] S.-Q. Yang, Y. Tao, P. Xu, and M. Chen, "Large-scale model experiment and numerical simulation on convergence deformation of tunnel excavating in composite strata," *Tunnelling and Underground Space Technology*, vol. 94, Article ID 103133, 2019.

[22] Q. S. Liu, P. H. Deng, C. Bi, W. W. Li, and J. Liu, "FDEM numerical simulation of the fracture and extraction process of soft surrounding rock mass and its rockbolt-shotcrete-grouting reinforcement methods in the deep tunnel," *Rock and Soil Mechanics*, vol. 40, no. 1, pp. 4065–4083, 2019.

[23] H. Y. Han, D. Fukuda, H. Y. Liu et al., "Combined finite-discrete element modellings of rockbursts in tunnelling under high in-situ stresses," *Computers and Geotechnics*, vol. 137, Article ID 104261, 2021.

[24] T. F. Ma, "Research on failure mechanism and supporting Technology for surrounding rock in soft rock roadways based on CDEM method," *Shanxi Coking Coal Science & Technology*, vol. 41, no. 11, pp. 43–47, 2019.

[25] L. T Peng, P. Lu, T. Yang, and C. D. Cheng, "Research on anti-water pressure capability of railway tunnel lining by continuous-discontinuous element method," *Journal of Chongqing University*, vol. 42, no. 11, pp. 98–107, 2019.

[26] Y. Ju, Y. Wang, C. Su, D. Zhang, and Z. Ren, "Numerical analysis of the dynamic evolution of mining-induced stresses and fractures in multilayered rock strata using continuum-based discrete element methods," *International Journal of Rock Mechanics and Mining Sciences*, vol. 113, pp. 191–210, 2019.

[27] C. Feng, Z. G. Li, and S. H. Li, "Study on uniaxial compression characteristics of brittle rock and soil aggregate," *Chinese Journal of Computational Mechanics*, vol. 35, no. 3, pp. 356–363, 2018.

[28] C. Feng, S. H. Li, B. X. Zheng, X. R. Cui, and J. J. Jia, "Numerical simulation on complete process of three-dimensional bench blasting in an open-pit mine based on CDEM," *Explosion and Shock Waves*, vol. 39, no. 2, pp. 110–120, 2019.
[29] C. Feng, S. H. Li, and J. Wang, "Stability analysis method for bedding rock slopes under seismic load," *Chinese Journal of Geotechnical Engineering*, vol. 34, pp. 717–724, 2012.
[30] C. Feng, S. H. Li, D. Zhou, and Q. B. Zhang, "Numerical analysis of damage and crack process of rock under explosive loading," *Chinese Journal of Geotechnical Engineering*, vol. 36, no. 7, pp. 1262–1270, 2014.
[31] C. Feng, S. H. Li, W. H. Hao, and W. Ge, "Numerical simulation for penetrating and blasting process of EPW based on CDEM," *Journal of Vibration and Shock*, vol. 36, no. 16, pp. 11–18, 2017.
[32] M. C. He and Z. B. Guo, "Mechanical property and engineering application of anchor bolt with constant resistance and large deformation," *Chinese Journal of Rock Mechanics and Engineering*, vol. 33, no. 7, pp. 1297–1308, 2014.
[33] Z. T. Wang, "Application of small diameter anchor cable in high in-situ stress and large deformation tunnel construction," *Tunnel construction*, vol. 25, no. 3, pp. 42–45, 2005.
[34] Z. D. Wu, H. W. Zhou, and J. F. Liu, "The application of steel fiber concrete in support of soft rock roadway at depth in the No.8 hebi coal mine," *Metal Mine*, vol. 6, no. 420, pp. 32–35, 2011.
[35] S. H. Zhong, *Promoting Effect of Shotcrete Anchor Support on Self-Supporting System in Surrounding Rock of Tunnel*, 1982.